LUND UNIVERSITY

Adaptive Interference Cancellation Using Common-Mode Information in DSL

Magesacher, Thomas; Ödling, Per; Börjesson, Per Ola

[Link to publication](#)

ADAPTIVE INTERFERENCE CANCELLATION USING COMMON-MODE INFORMATION IN DSL

Thomas Magesacher, Per Ödling, and Per Ola Börjesson

Department of Information Technology, Lund University
P.O. Box 118, S-22100 Lund, Sweden
email: tom@it.lth.se

ABSTRACT

Exploiting the common-mode (CM) receive signal in wireline communication can yield significant improvements in terms of channel capacity compared to using only the differential-mode (DM) signal. Recently published, independent, scientific work proposed the employment of an adaptive CM-reference based interference canceller and reported performance improvements based on simulation results. Adaptive processing of correlated receive signals, however, bears the potential danger of cancelling the useful component—an undesired effect we will address.

We present an analysis of the linear adaptive cancellation approach in this application. For a large class of practically relevant cases, it can be shown that a canceller, whose coefficients are adapted while the far-end transmitter is silent, yields a signal-to-noise-and-interference power ratio (SNIR) which is higher than the SNIR of the DM-only channel output. Moreover, the performance of a canceller with this tap-setting is close to the performance of the front-end that is optimum in the sense of maximising the SNIR at its output. Adaptation while the useful far-end signal is present yields a front-end whose output SNIR is considerably lower compared to the SNIR of the DM channel output. The results and their practical impact are demonstrated by an example.

1. INTRODUCTION

Communications over copper cables is conventionally carried out by differential signalling. On physical-layer level, this corresponds to transmitting a signal x as a voltage applied between the two wires of a pair. The differential-mode (DM) signal at the receive side, denoted by y_1 in Figure 1, is derived from the voltage measured between the two wires. DM signalling over twisted-wire pairs, patented by Alexander Graham Bell more than hundred years ago [1], exhibits a high degree of immunity against ingress of unwanted interference, caused, for example, by radio transmitters (radio frequency interference) or by data transmission in neighbouring pairs (crosstalk). The performance of almost all high-datarate (and thus also high-bandwidth consuming) digital subscriber line (DSL) systems is limited by crosstalk.

Cable investigations indicate that the number of strong crosstalk sources is often very low in practice—one, two or maybe three dominant crosstalkers significantly raise the crosstalk noise level and thus reduce the performance on the pair under consideration [2]. In such cases, it is beneficial to exploit the common-mode (CM) signal y_2, which is the signal corresponding to the arithmetic mean of the two voltages measured between each wire and earth, at the receive side. The CM signal and the DM signal of a twisted-wire pair are strongly correlated. Exploiting the CM signal in addition to the DM signal yields a new composite channel whose capacity can be, depending on the scenario, up to three times higher than the conventional, DM-only channel capacity [3, 4]. The large benefit is

achieved for exactly those scenarios that are challenged by strong interference.

Independent scientific work [5, 6] suggests the employment of an interference canceller whose output at time-instant n is given by

$$y[n] = y_1[n - D] + h_k[n] * y_2[n], \qquad (1)$$

where $*$ denotes linear convolution, D specifies the delay of y_1 in samples and $h_k[n], 0 \le n \le N-1$ are the coefficients of a linear adaptive filter whose input is the CM signal y_2, as depicted in Figure 1. Adaptive processing of correlated receive signals bears the potential danger of cancelling the useful component. Despite the performance improvements reported in [5, 6], it is *a priori* not clear whether the proposed kind of adaptive interference cancellation is beneficial or counter-productive.

This paper investigates the receiver front-end for CM-aided wireline transmission. Section 2 introduces a suitable channel model in the discrete Fourier transform (DFT) domain, which allows us to carry out the analysis on subchannel level. Based on experience gained from measurements, Section 3 identifies some channel characteristics which hold for a large set of applications. A part of the analysis presented in Section 4 is based on these assumptions. The performance of an adaptive scheme based on a squared error criterion (LMS, RLS), *i.e.*, the *ad hoc* solution proposed in [5, 6], is investigated using the Wiener filter solution. Section 5 presents numerical results for a DSL application frequently encountered in practice and Section 6 concludes the paper.

2. CHANNEL MODEL

The single-user wireline channel can be modelled as a linear stationary Gaussian vector channel with memory and coloured interference, *i.e.*, the interference is correlated in time. In the following, we restrict ourselves to a single interference source, which typically models the strongest far-end crosstalk (FEXT) or near-end crosstalk (NEXT) disturber. Figure 1 depicts a block diagram of the channel and of the interference canceller. The DM output $y_1[n]$ and the CM
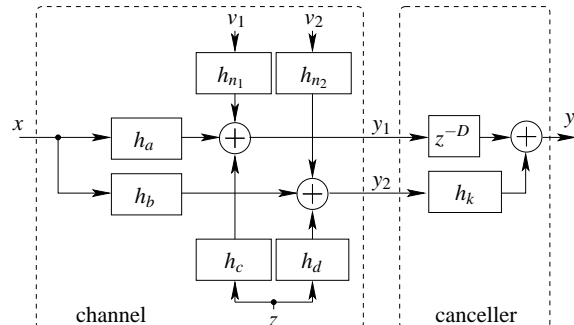

Figure 1: Block diagram of the channel model (2) and the linear interference canceller (1).

output $y_2[n]$ of a twisted-wire pair at time instant n are given by

$$\begin{bmatrix} y_1[n] \\ y_2[n] \end{bmatrix} = \begin{bmatrix} h_a[n] \\ h_b[n] \end{bmatrix} * x[n] + \begin{bmatrix} h_c[n] & h_{n_1}[n] & 0 \\ h_d[n] & 0 & h_{n_2}[n] \end{bmatrix} * \begin{bmatrix} z[n] \\ v_1[n] \\ v_2[n] \end{bmatrix} \quad (2)$$

for $-\infty \leq n \leq \infty$, where $h_a[n], h_b[n], h_c[n], h_d[n], h_{n_1}[n], h_{n_2}[n]$ are time-invariant impulse responses and $x[n], z[n], v_1[n], v_2[n]$ denote transmit signal, interference, DM noise and CM noise at time instant n, respectively. All signals and all impulse responses are real-valued. We denote the length of the longest impulse response involved in (2) by M and assume that the sequences $\{x[n]\}_{-\infty \leq n \leq \infty}$, $\{z[n]\}_{-\infty \leq n \leq \infty}$, $\{v_1[n]\}_{-\infty \leq n \leq \infty}$, and $\{v_2[n]\}_{-\infty \leq n \leq \infty}$ are mutually independent and consist of independent, identically distributed, real-valued, zero-mean, unit-variance Gaussian random variables. Both colouring and power scaling can be incorporated in the filters.

Following the technique used in [7], we extend the impulse responses $h_a[n], h_b[n], h_c[n], h_d[n], h_{n_1}[n], h_{n_2}[n]$ with zeros such that the resulting responses $\tilde{h}_a[n], \tilde{h}_b[n], \tilde{h}_c[n], \tilde{h}_d[n], \tilde{h}_{n_1}[n], \tilde{h}_{n_2}[n]$ all have length N, where N is chosen such that $N \geq M$. The observation of a block of N samples yields the modified channel model

$$\begin{bmatrix} \tilde{y}_1[n] \\ \tilde{y}_2[n] \end{bmatrix} = \sum_{i=0}^{N-1} \begin{bmatrix} \tilde{h}_a[i] \\ \tilde{h}_b[i] \end{bmatrix} x[(n-i)_N] + \sum_{i=0}^{N-1} \begin{bmatrix} \tilde{h}_c[i] & \tilde{h}_{n_1}[i] & 0 \\ \tilde{h}_d[i] & 0 & \tilde{h}_{n_2}[i] \end{bmatrix} \begin{bmatrix} z[(n-i)_N] \\ v_1[(n-i)_N] \\ v_2[(n-i)_N] \end{bmatrix}, \quad (3)$$

where $0 \leq n \leq N-1$ and $(\cdot)_N$ denotes addition modulo N. This N-circular channel is equivalent to the channel defined in (2) in the sense that it has, in the limit for $N \rightarrow \infty$, the same capacity under a per-symbol average energy constraint [7]. Taking the N-point DFT[1] of (3) yields

$$\begin{bmatrix} Y_1[m] \\ Y_2[m] \end{bmatrix} = \begin{bmatrix} a[m] \\ b[m] \end{bmatrix} X[m] + \begin{bmatrix} c[m] & n_1[m] & 0 \\ d[m] & 0 & n_2[m] \end{bmatrix} \begin{bmatrix} Z[m] \\ V_1[m] \\ V_2[m] \end{bmatrix}, \quad (4)$$

for $0 \leq m \leq N-1$, where $Y_1[m], Y_2[m], a[m], b[m], X[m], c[m], d[m], n_1[m], n_2[m], Z[m], V_1[m], V_2[m]$ are the N-point DFTs of $\tilde{y}_1[n], \tilde{y}_2[n], \tilde{h}_a[n], \tilde{h}_b[n], x[n], \tilde{h}_c[n], \tilde{h}_d[n], \tilde{h}_{n_1}[n], \tilde{h}_{n_2}[n], z[n], v_1[n], v_2[n]$, respectively. The DFT-domain model (4) describes N parallel, independent and in general complex-valued subchannels, where the first $\lfloor N/2 \rfloor + 1$ subchannels with indices $0 \leq m \leq \lfloor N/2 \rfloor$ are independent and the remaining $\lceil N/2 \rceil - 1$ subchannels with indices $\lfloor N/2 \rfloor + 1 \leq m \leq N-1$ are redundant. The DFT-domain model (4) allows us to continue the investigation on subchannel level. In the following, we omit the subchannel index m wherever possible for the sake of simple notation.

3. CHANNEL PROPERTIES

Based on cable models [2, 8, 9, 10] and on experience from measurements [3, 11], we observe that a large class of scenarios with practical relevance obeys the following conditions ($|\cdot|$ denotes absolute value):

Assumption 1 $|a| \overset{(\alpha)}{\gg} |b| \overset{(\beta)}{\approx} |c| \overset{(\gamma)}{\approx} |d| \overset{(\delta)}{\gg} |n_2| \overset{(\varepsilon)}{\approx} |n_1|.$

For FEXT, (α) always holds since the model for the FEXT coupling function includes scaling by the insertion loss of the line. For NEXT, in systems with overlapping frequency bands for upstream and downstream, (α) does not necessarily hold for long loops and/or high frequencies since the NEXT coupling function is virtually independent of the loop length [9]. Consequently, the level of the receive signal power spectral density (PSD) on long loops may be lower than the NEXT PSD level. Most high-bandwidth

---

[1]The N-point DFT $\mathbf{X} = \begin{bmatrix} X[0] & \cdots & X[N-1] \end{bmatrix}^T$ of the signal $\mathbf{x} = \begin{bmatrix} x[0] & \cdots & x[N-1] \end{bmatrix}^T$ is given by $\mathbf{X} = \mathbf{F}\mathbf{x}$, where $(\mathbf{F})_{n,k} = \exp(-j2\pi nk/N), \quad 0 \leq n,k \leq N-1.$
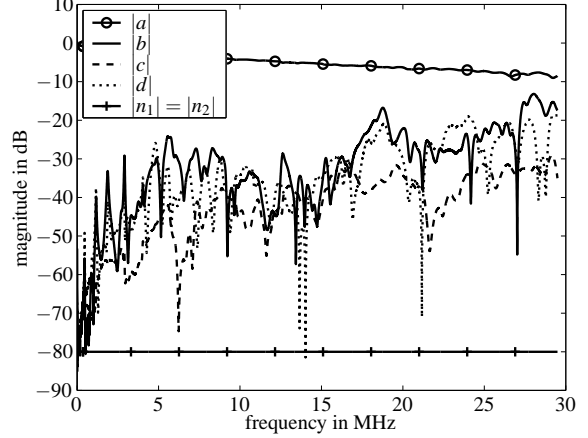

Figure 2: Channel properties a, b, c, d obtained from measurements. The y-axis denotes relative magnitude in dB. Assuming a VDSL transmit power spectral density of $-60\,\text{dBm/Hz}$ results in a level of $-80\,\text{dB}$ for n_1 and n_2 in order to obtain a background noise power spectral density (PSD) of $-140\,\text{dBm/Hz}$, which is the level suggested in standardisation documents [9, 10].

consuming DSLs, however, employ frequency division duplexing and are thus only vulnerable to alien NEXT, i.e., NEXT from systems of different types, and "out-of-band self-NEXT", i.e., NEXT caused by the out-of-band transmit signals of systems of the same type. Alien NEXT is often taken care of by spectral management. Self-NEXT is usually negligible due to out-of-band spectral masks.

Relations (β) and (γ) are mainly based on measurement experience [3, 11]. While (δ) always holds for NEXT, it may not be true for FEXT on long loops, where the FEXT PSD levels are pushed below the background noise PSD levels due to loop attenuation. Relation (ε), which implies that the CM background noise level is of the same order of magnitude as the DM background noise level, is not vital for the analysis. The CM background noise level should, however, be low enough such that (δ) is justified, which is a reasonable assumption although the CM background noise level may be a bit higher than the DM background noise level. Figure 2 shows exemplary channel transfer functions based on measurements [3]. Assumption 1 holds for almost the whole frequency range in this case.

To conclude, Assumption 1 is valid for frequency division duplexed systems as long as the pair under consideration and the crosstalk-causing pair have roughly the same length and are neither extremely short nor extremely long. In case the pairs are extremely short, the crosstalk PSD levels are very low and consequently (β) does not hold. In case the pairs are extremely long, both the crosstalk PSD levels and the receive signal PSD levels are very low, which may lead to neither (α) nor (β) being true. Cases with extreme lengths (short or long) are of little practical interest, since extremely short loops are not found in the field and extremely long loops are out of scope for high-bandwidth consuming DSL techniques. Care should be taken with near/far scenarios for which, typically, (α) does not hold since the useful signal is severely attenuated while the crosstalk is strong. However, near/far problems are often handled by power cut-back schemes.

4. ANALYSIS

4.1 Maximum likelihood (ML) based canceller

It can be shown that the ML estimator for the DFT-domain transmit signal $X[m]$ suggests a linear combination of $Y_1[m]$ and $Y_2[m]$. Except for a scaling factor, this ML estimator has the structure of a linear interference canceller yielding the output

$$Y^{(\text{ML})}[m] = Y_1[m] + k^{(\text{ML})}[m]Y_2[m].$$

The coefficient $k^{(\text{ML})}[m]$ is given by

$$k^{(\text{ML})}[m] = \frac{b'[m](|c[m]|^2+|n_1[m]|^2) - a'[m]c[m]d'[m]}{a'[m](|d[m]|^2+|n_2[m]|^2) - b'[m]c'[m]d[m]}, \quad (5)$$

where $\cdot'$ denotes complex conjugate.

Note that $k^{(\text{ML})}[m]$ is the interference canceller coefficient for which the mutual information $I(X[m];Y^{(\text{ML})}[m])$ of $X[m]$ and the canceller output $Y^{(\text{ML})}[m]$ is maximised. Furthermore, $I(X[m];Y^{(\text{ML})}[m])$ is equal to the mutual information $I(X[m];Y_1[m],Y_2[m])$ of the transmit signal $X[m]$ and the receive signal pair $(Y_1[m],Y_2[m])$, i.e., $I(X[m];Y^{(\text{ML})}[m]) = I(X[m];Y_1[m],Y_2[m])$. The ML-based canceller preserves the information contained in the two channel output signals. Consequently, $Y^{(\text{ML})}[m]$ is also the output that maximises the signal-to-noise-and-interference power ratio (SNIR) in each subchannel. The corresponding ML-based time-domain coefficients $h_k[n]$ of the canceller described by (1) are given by the inverse DFT

$$\left[h_k^{(\text{ML})}[0] \; \cdots \; h_k^{(\text{ML})}[N-1]\right]^{\text{T}} = \mathbf{F}^{-1}\left[k^{(\text{ML})}[0] \; \cdots \; k^{(\text{ML})}[N-1]\right]^{\text{T}}. \quad (6)$$

4.2 Adaptive canceller

In the following, the suitability of adaptive cancellation schemes based on a squared error criterion is investigated. Popular examples of such schemes are the least-mean square (LMS) and the recursive least squares (RLS) algorithm. In a stationary environment, these algorithms can be parameterised so that they converge to a solution which is arbitrarily close to the Wiener filter solution.

The Wiener filter solution $k^{(\text{LMS1})}[m]$ for $X[m]\neq 0$, which is the solution a properly parameterised algorithm converges to when the coefficients are adapted *while the useful far-end signal x is present*, is given by

$$k^{(\text{LMS1})}[m] = \arg\min_k \mathrm{E}\left(Y^2[m]\right) = -\frac{a[m]b'[m]+c[m]d'[m]}{|b[m]|^2+|d[m]|^2+|n_2[m]|^2}. \quad (7)$$

The Wiener filter solution $k^{(\text{LMS2})}[m]$ for $X[m]=0$, which is the solution a properly parameterised algorithm converges to when the coefficients are adapted *while there is no useful far-end signal x*, is given by

$$k^{(\text{LMS2})}[m] = \arg\min_k \mathrm{E}\left(\left.Y^2[m]\right|_{X[m]=0}\right) = -\frac{c[m]d'[m]}{|d[m]|^2+|n_2[m]|^2}. \quad (8)$$

We use the mutual information of $X[m]$ and $Y_1[m]$, which can be written as

$$I(X[m];Y_1[m]) = \frac{1}{2}\log_2\left(1+\frac{|a[m]|^2}{|c[m]|^2+|n_1[m]|^2}\right),$$

in order to assess the performance of the adaptive algorithms.

Proposition 1 *Under the conditions defined in* Assumption 1, *the following inequality holds:*

$$I(X[m];Y^{(\text{LMS1})}[m]) \leq I(X[m];Y_1[m]), \quad 0 \leq m \leq N-1.$$

In other words, in each subchannel the SNIR of the output $Y^{(\text{LMS1})}$ of a linear interference canceller with tap setting $k^{(\text{LMS1})}$ given by (7) is lower than the SNIR of Y_1. Consequently, the SNIR of the output $y^{(\text{LMS1})}$ of the interference canceller (1) with coefficients set to

$$\left[h_k^{(\text{LMS1})}[0]\cdots h_k^{(\text{LMS1})}[N-1]\right]^{\text{T}} = \mathbf{F}^{-1}\left[k^{(\text{LMS1})}[0]\cdots k^{(\text{LMS1})}[N-1]\right]^{\text{T}} \quad (9)$$

is lower than the SNIR of the DM-output y_1.

Motivation: Since the strongest component in Y_1 stems from X, there is a mechanism driving the canceller coefficient towards $-a/b$, which is the coefficient that eliminates X (note that $|a/b| \gg 1$). Since increasing $|k|$ increases the residual of Z in Y, there is a counter mechanism working against large values of $|k|$. These two mechanisms reach an equilibrium for the solution given by (7). The net result is that the power of X in $Y^{(\text{LMS1})}$ is reduced (compared to Y_1), which implies $|k^{(\text{LMS1})}| \gg 1$. However, the larger $|k^{(\text{LMS1})}|$, the higher the power of the Z-component in $Y^{(\text{LMS1})}$ compared to Y_1. More precisely, for any $k^{(\text{LMS1})}$ that fulfils $|k^{(\text{LMS1})}| > 2$, the power of the Z-component in $Y^{(\text{LMS1})}$ is higher than in Y_1. To summarise, while the power of the X-component is lower in $Y^{(\text{LMS1})}$ compared to Y_1, the power of the Z-component is higher in $Y^{(\text{LMS1})}$ compared to Y_1, which confirms Proposition 1.

Proposition 2 *Under the conditions defined in* Assumption 1, *the following inequality holds:*

$$I(X[m];Y^{(\text{LMS2})}[m]) \geq I(X[m];Y_1[m]), \quad 0 \leq m \leq N-1.$$

In other words, in each subchannel the SNIR of the output $Y^{(\text{LMS2})}$ of a linear interference canceller with tap setting $k^{(\text{LMS2})}$ given by (8) is higher than the SNIR of Y_1. Consequently, the SNIR of the output $y^{(\text{LMS2})}$ of the interference canceller (1) with coefficients set to

$$\left[h_k^{(\text{LMS2})}[0]\cdots h_k^{(\text{LMS2})}[N-1]\right]^{\text{T}} = \mathbf{F}^{-1}\left[k^{(\text{LMS2})}[0]\cdots k^{(\text{LMS2})}[N-1]\right]^{\text{T}} \quad (10)$$

is higher than the SNIR of the DM-output y_1.

Motivation: Since the strongest component in Y_1 stems from Z, the Wiener filter solution is close to $-c/d$ (the exact solution is given by (8)), which essentially eliminates the component of Z. Since $|k^{(\text{LMS2})}| \approx |c/d| \approx 1$, the power of the V_2-component in $Y^{(\text{LMS2})}$ remains negligible. A lower and an upper bound for the signal energy (i.e., energy of X) contained in $Y^{(\text{LMS2})}$ are $|a|^2 - |b|^2$ and $|a|^2 + |b|^2$, respectively. Consequently, the front-end may cause a negligible reduction of signal power ($|b| \ll |a|$) while essentially eliminating the interference. Thus, its performance is close to that of the ML-estimator.

Note that the time-domain solutions $h_k^{(\text{ML})}$, $h_k^{(\text{LMS1})}$ and $h_k^{(\text{LMS2})}$ given by (6), (9) and (10), respectively, are in general non-causal. A real-time implementation of the canceller thus requires the delay of y_1, as indicated in Figure 1.

The conclusion drawn from Proposition 1 and Proposition 2 for a typical wireline scenario (typical in the sense that Assumption 1 is valid) with one dominant crosstalker, is the following: A canceller set to the Wiener filter solution $k^{(\text{LMS2})}$ (i.e., adaptation is performed while the transmitter is silent) exhibits a higher SNIR at the output compared to the DM channel output. Moreover, its performance is close to the ML estimator's performance. A canceller set to the Wiener filter solution $k^{(\text{LMS1})}$ (i.e., adaptation is performed while the transmitter is active) exhibits a lower SNIR at the output compared to the DM channel output.

5. EXAMPLE

The practical impact of the insights gained in the previous section is best demonstrated by an example. The following scenario focuses on very high data rate DSL (VDSL) transmission, which exploits the frequency range up to 12 MHz according to the current status of standardisation [9, 10]. The setup addresses the near-far problem in upstream (US) direction that occurs when deploying VDSL from the central office to both distant and nearby customers, as depicted in Figure 3. In our example, an upstream transmission from customer A over a loop of length 1000 m is disturbed by strong crosstalk from customer B, which is 250 m away from the central office. We assume a background noise level of -130 dBm/Hz at
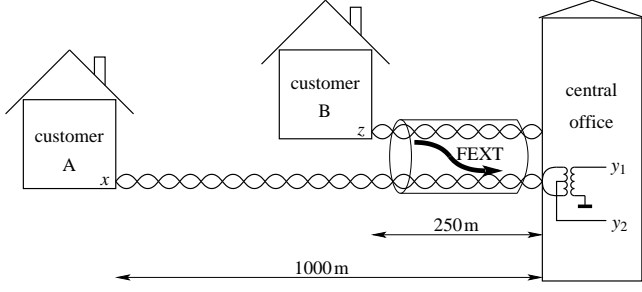
Figure 3: Example scenario: VDSL upstream (US) transmission from customer A to the central office over a twisted pair of length 1000 m with a self-FEXT disturber (customer B) located at a distance of 250 m from the central office.
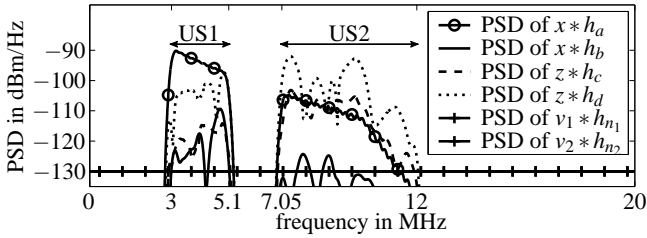

Figure 4: PSDs of signal (solid line marked with circles: DM port; solid line: CM port), interference (dashed line: DM port; dotted line: CM port) and background noise (solid lines marked with plus signs) at the receiver input. Assumption 1 is essentially valid for a large portion of the US1 band but does not hold at all for the US2 band.

both the CM and the DM port. According to the standardised frequency plan, two bands are used: the lower band US1 from 3 MHz to 5.1 MHz and the upper band US2 from 7.05 MHz to 12 MHz. This near-far example is very suitable for demonstration purposes since it has the property that the essential parts of Assumption 1, *i.e.*, (α) and (ε), hold for a wide part of US1 while Assumption 1 does not hold at all for US2, as the PSDs depicted in Figure 4 show. We choose a flat background noise PSD at both the DM and the CM port of -130 dBm/Hz, since practical experience indicates that the value of -140 dBm/Hz proposed in standards may be too optimistic.

Table 1 summarises the resulting datarates, where apart from the total rate in US direction, also the rates achieved in the lower and in the upper band are presented. A comparison of the maximum datarates $I(x; y_1)$ and $I(x; y_1, y_2)$ using DM and both DM and CM, respectively, shows the potential of CM-aided reception. In particular, in the US2 band, the maximum CM-DM datarate of 24.30 Mbit/s is about eight times higher than the maximum DM-datarate of 3.49 Mbit/s. Note that the maximum CM-DM datarate $I(x; y_1, y_2) = I(x; y^{(\mathrm{ML})})$ is obtained from the solution for the coefficients given by (5) and (6).

For the US1 band, we observe that a receiver employing a can-

	US1	US2	US
max. DM rate $I(x; y_1)$	17.11	3.49	20.60
rate $I(x; y^{(\mathrm{LMS1})})$ using $h_k^{(\mathrm{LMS1})}$	11.94	23.21	35.15
rate $I(x; y^{(\mathrm{LMS2})})$ using $h_k^{(\mathrm{LMS2})}$	24.88	24.30	49.18
max. DM-CM rate $I(x; y_1, y_2)$	24.88	24.30	49.18

Table 1: Datarates in Mbit/s achieved in the lower US band (US1), in the higher US band (US2) and in total (sum of the rates in US1 and US2).

celler adjusted to $h_k^{(\mathrm{LMS1})}$ achieves a datarate which is substantially lower compared to exploiting the DM-output only. Employing a canceller set to $h_k^{(\mathrm{LMS2})}$, on the other hand, yields a datarate which is extremely close to the maximum DM-CM rate of 24.88 Mbit/s. These observations are in accordance with the propositions presented above.

In the US2 band, both cancellers perform reasonably well since the PSD of the signal component $x * h_b$ present at the CM-port drowns in the background noise $v_2 * h_{n_2}$ (cf. Figure 4). Note that neither Proposition 1 nor Proposition 2 can be applied for the US2 band since Assumption 1 does not hold.

From the total US datarate, which is just the sum of the rates achieved in the two bands, we observe that it is possible to obtain an improvement in datarate using a canceller $h_k^{(\mathrm{LMS2})}$, although such a canceller actually lowers the datarate in the band US1.

6. SUMMARY AND CONCLUSIONS

This paper investigates the receiver front-end for CM-aided wireline transmission. A set of wireline channel properties that hold in most practical cases has been identified and summarised. Based on these assumptions, we conclude that the coefficients of an interference canceller should be adapted while the far-end transmitter is silent. The performance under these conditions is close to the ML estimator's performance. Furthermore, a canceller adapted while the transmitter is active, lowers the performance of the receiver compared to exploiting only the DM channel output.

REFERENCES

[1] A. G. Bell, "Improvement in Telegraphy," *Letters Patent No. 174,465, dated March 7, application filed February 14*, 1876.

[2] T. Starr, J. M. Cioffi, and P. Silverman, *Understanding Digital Subscriber Line Technology*, Prentice Hall, Englewood Cliffs, 1998.

[3] T. Magesacher, P. Ödling, P. O. Börjesson, W. Henkel, T. Nordström, R. Zukunft, and S. Haar, "On the Capacity of the Copper Cable Channel Using the Common Mode," in *Proc. Globecom 2002*, Taipei, Taiwan, Nov. 2002.

[4] T. Magesacher, P. Ödling, P. O. Börjesson, and S. Shamai (Shitz), "Information Rate Bounds in Common-Mode Aided Wireline Communications," *to appear in European Transactions on Telecommunications (ETT)*, 2005.

[5] T. H. Yeap, D. K. Fenton, and P. D. Lefebvre, "A Novel Common-Mode Noise Cancellation Technique for VDSL Applications," *IEEE Trans. Instrum. and Measurement*, vol. 52, no. 4, pp. 1325–1334, Aug. 2003.

[6] A. H. Kamkar-Parsi, M. Bouchard, G. Bessens, and T.H. Yeap, "A Wideband Crosstalk Canceller for xDSL Using Common-Mode Information," *IEEE Trans. Commun.*, vol. 53, no. 2, pp. 238–242, Feb. 2005.

[7] W. Hirt and J. L. Massey, "Capacity of the Discrete-Time Gaussian Channel with Intersymbol Interference," *IEEE Trans. Inform. Theory*, vol. 34, no. 3, pp. 380–388, May 1988.

[8] W. Y. Chen, *DSL: Simulation Techniques and Standards Development for Digital Subscriber Line Systems*, Macmillan Technical Publishing, ISBN 1-57870-017-5, 1998.

[9] ETSI TM6, "Transmission and Multiplexing (TM); Access Transmission Systems on Metallic Access Cables; Very high speed Digital Subscriber Line (VDSL); Part 1: Functional requirements," *TS 101 270-1, Version 1.1.6*, Aug. 1999.

[10] ANSI T1E1.4, "Very-high-bit-rate Digital Subscriber Line (VDSL) Metallic Interface Part 1: Functional Requirement and Common Specification," *T1E1.4/2000-009R3*, Feb. 2001.

[11] T. Magesacher, W. Henkel, G. Tauböck, and T. Nordström, "Cable Measurements Supporting xDSL Technologies," *Journal e&i Elektrotechnik und Informationstechnik*, vol. 199, no. 2, pp. 37–43, Feb. 2002.